Construction and Building Materials 93 (2015) 309–316

Contents lists available at ScienceDirect

Construction and Building Materials

journal homepage: www.elsevier.com/locate/conbuildmat

Preparation and characterization of granular silica aerogel/polyisocyanurate rigid foam composites

Chunying Zhao, Yun Yan *, Zhihua Hu, Liping Li, Xiaozheng Fan

[a] State Key Laboratory Cultivation Base for Nonmetal Composites and Functional Materials, Southwest University of Science and Technology, Mianyang, SiChuan 621010, PR China
[b] Key Laboratory for Advanced Building Materials of SiChuan Province, Southwest University of Science and Technology, Mianyang, SiChuan 621010, PR China

HIGHLIGHTS

- A new polyisocyanurate/granular silica aerogel composite rigid foam was prepared.
- The novel organic/inorganic composite rigid foam has the remarkable performances.
- Waste residue was used to replace partially polyols to effectively save the cost.

ARTICLE INFO

Article history:
Received 14 January 2015
Received in revised form 3 May 2015
Accepted 27 May 2015
Available online 11 June 2015

Keywords:
PIR rigid foam
Granular silica aerogel
Composite foam
Flame retardant
Thermal insulation performance

ABSTRACT

Energy conservation is an increasingly important issue in building and construction. Consequently, thermal insulation of building materials, particularly insulation systems for external walls, has attracted increasing attention in recent years. A novel organic/inorganic composite rigid foam (polyisocyanurate and granular silica aerogel) with excellent flame retardant and thermal insulation properties has been synthesized. The effects of granular silica aerogel and polymer polyols on the performance of composites were characterized using scanning electron microscopy (SEM), oxygen index (OI), thermal conductivity and mechanical evaluation. The OI value of the composite foam prepared with polyethylene glycol 600 increased from 29.4% (0 wt.% aerogel) to 34.6% (8 wt.% aerogel), indicating improved thermal stability, and thermal conductivity was reduced by 32.7% (0.0233 W/(m K) at 8 wt.% aerogel) compared with polyisocyanurate (PIR) rigid foam (0.0346 W/(m K)). Waste residue (a by-product from the preparation of 1,4-butanediol) was successfully used to partially replace the polyol source in order to effectively reduce costs.

1. Introduction

Since building energy consumption (BEC) accounts for a large proportion of global total energy consumption, increasing BEC has become a critical problem for contemporary society [1–3]. To address this, energy saving materials that can improve the energy efficiency of a building and reduce BEC have attracted widespread interest [4,5]. Since the energy efficiency of buildings is greatly reliant on reducing heat transfer through selection of building envelopes and their components, external thermal insulation of building walls has been regarded as effective [6,7]. Thermal insulation, as a major contributor, is clearly the first practical and logical step towards achieving energy efficiency [1]. Moreover, thermal insulation of building walls significantly reduces thermal energy consumption, resulting in lower carbon dioxide (CO_2) emissions. As a least-cost energy strategy, thermal insulation of a building external wall can be seen as an investment in economic terms [8].

As for the thermal insulating materials for exterior walls of buildings, polyisocyanurate (PIR) rigid foam is one of rigid polyurethane foam (RPUF) modified. RPUF is a closed-cell plastic and one of the most efficient, high performance insulation material, enabling very effective energy savings with minimal occupation of space (2 opinions for Reviewer #2). PIR rigid foam is a cost-effective solution because it has low thermal conductivity, closed-cell structure, excellent adhesion and superior mechanical properties, unmatched by any other conventional product [9,10]. In addition, PIR rigid foam is stable and durable. It offers optimal insulation and has a useful life exceeding 50 years. PIR rigid foam provides effective energy savings with minimal space consumption and is one of the most efficient, high-performance insulating materials available [11]. However, PIR rigid foam also has some

* Corresponding author at: State Key Laboratory Cultivation Base for Nonmetal Composites and Functional Materials, Southwest University of Science and Technology, Mianyang, SiChuan 621010, PR China.
E-mail address: yanyun@swust.edu.cn (Y. Yan).

http://dx.doi.org/10.1016/j.conbuildmat.2015.05.129
0950-0618/

disadvantages, such as poor thermal stability, high flammability and susceptibility to degradation upon exposure to elevated temperatures during fire, which constitute serious concerns and heavily hinder its practical application. A great deal of effort has been devoted to modification of PIR to improve its flame retardant properties and increase its utility [12,13]. Considerable attention has been devoted to the combination of PIR rigid foam with inorganic materials by many academic and industrial researchers, but so far with limited success [14].

Recently, numerous studies on polyurethane (PU)/inorganic composites have been reported [12], including the use of carbon nanotubes, expandable graphite, calcium carbonate, and organically-modified montmorillonites [15–18]. RPUF nano-composites, which combine RPUF with inorganic nanoparticles, have attracted the attention of many researchers since they exhibit enhanced mechanical, thermal and flame retardant properties [19]. Whilst addition of inorganic material to RPUF can improve flame retardant properties, the resulting composites are not good thermal insulators because of the high thermal conductivity, density and water absorption of the inorganic materials. It is difficult to produce monodispersed nanoparticles in a polymer matrix due to agglomeration as a result of the specific surface area and volume of the nanoparticles. Even if agglomeration can be overcome by modification of the surface of the inorganic particles, cost of production is relatively high [20].

Recently, inorganic nanoporous materials such as aerogels, which can provide excellent thermal insulation, have been used in composite systems [21]. Silica aerogels are ultra-light materials with high porosity, high surface area and excellent adiabatic performance that have great potential as thermal insulation materials [13]. Because of their hydrophobicity, silica aerogels are relatively easy to disperse and have become the most promising high thermal insulation materials for building applications today [22,23]. However, a major disadvantage of aerogels as insulation materials is that they are brittle, which has greatly restricted their application as thermal insulators.

In this study, new composite organic/inorganic foams were prepared. PIR rigid foam was combined with granular silica aerogels by a step hybrid method, which was expected to provide efficient energy-saving composite materials. These new composites have excellent adiabatic performance, low thermal conductivity and are either flame retardant or non-combustible. Their properties give them excellent potential in the field of thermal insulation to provide building energy efficiency and fire prevention.

2. Experimental

2.1. Materials

The raw materials employed in polyurethane foam synthesis were as follows: polyether polyols MA-4110 (hydroxyl value 430 ± 20 mgKOH/g); phthalic anhydride polyester polyol (polyester polyol PS-3152), (hydroxyl value 300–330 mgKOH/g); polyethylene glycol (PEG) 600 (AR, molecular weight 570–630); waste residue, a complex polyol polymer, was a by-product from the preparation of 1,4-butanediol, its content includes C(51.88%), H(6.462%), Na_2O(81.64%), Fe_2O_3(11.31%), CaO(3.6%) and Cl(1.38%) through the analysis (3 opinions for Reviewer #2); polyaryl polymethylene isocyanate (PAPI: Polymeric MDI (diphenylmethane diisocyanate) Bayer 44v20) (NCO: 30.5–32.0%, average functionality: 2.8, viscosity at 25 °C: 150–250 mPa s, purity ⩾ 99.6%); silicone surfactant: SD-611; flame retardant: dimethyl methylphosphonate; blowing agent: blend of 1,1-dichloro-1-fluoroethane (HCFC-141B), (purity > 98%), and catalyst: K-15 (potassium octanoate solution 70%); granular silica aerogel with hydrophobic properties was prepared at Southwest University of Science and Technology. The steps of making the hydrophobic silica aerogel are as follows. A certain concentration of solution was obtained from sodium silicate and hydrochloric acid and then made it static gel in a certain temperature by adjusting pH value. Gel was gradually aging by adding the aging medium under certain of conditions. And then gel proceed a solvent replacement with *n*-hexane. The surface of gel had modified with a silane coupling agent into hydrophobic gel (3 opinions for Reviewer #2). Properties of the silica aerogel were as follows: specific surface area (600–800 m^2/g), thermal conductivity (0.017–0.021 W/(m K)), pore size (5–100 nm), total porosity (90 vol%). Macroscopic and microscopic images of the granular silica aerogel are shown in Fig. 1.

2.2. Preparation of PIR composites

Two components, A and B, were prepared. Component A was a mixture containing polyols, catalyst, blowing agent, surfactant and flame retardant. Component B was PAPI.

The foams were prepared by the one-shot and free-rise method in a single step from a two-component (A and B) system. All components of A were firstly mixed well in a beaker and stirred together at ambient temperature for 20 min with an electric stirrer until a uniform mixture was obtained. The different dosage (1%, 2%, 3%, 4%, 5%, 6%, 8%) (6 opinions for Reviewer #2) of granular silica aerogel was added to the matrix with stirring using a high speed (2500 rpm) mechanical stirrer. After 30 min, PAPI was added to the mixture in a defined weight ratio and the reaction was allowed to proceed at room temperature with vigorous stirring for 30 s. The resultant mixture was immediately poured into an open mold (100 × 100 × 50 cm) to produce free-rise foam and cured for 15 min at room temperature. The PIR composite foams were cured at room temperature for 15 min. In order to increase the crosslink density and make the reaction more sufficient, the synthesized PIR composite foams were put into an oven and heat-treated at 60 °C for 48 h after demoulding. Different test samples of defined shapes were cut from the cured foam. Dimensional finishing was completed by rubbing with fine emery paper.

2.3. Characterization

2.3.1. Mechanical properties of PIR composite foams

The compressive strengths of the PIR foams were measured using a WSM-10KN universal mechanical tester at 25 °C and 45% relative humidity. A foam sample was cut into a 100 × 100 mm block with a thickness of 50 mm. The strength test was performed using a displacement speed of 5 mm/min. Compressive strength (*r*, Pa) was calculated according to GB/T 8813-2008 standards. Five replicates were recorded for each PIR composite foam sample.

2.3.2. Thermal performance by thermogravimetric analysis (TGA)

Thermal analyses of the PIR foams were carried out on a TGA/SDTA851e instrument to study decomposition of the foam at distinct phases. Approximately 5 mg of sample was placed on the platinum pan before it was put in the furnace. TGA runs were conducted in ramp mode over a temperature range of 30–800 °C under a dry nitrogen flow of 50 ml/min at a heating rate of 20 °C/min.

2.3.3. Oxygen index (OI) of PIR composite foams

Flame retardant test: OI testing was carried out according to GB/T2406-1993 to determine the relative flammability of foam using an LFY-606 OI instrument. The quintessential feature of OI methods is that the sample is burnt within a controlled atmosphere. The standard procedure is to ignite the top of the sample to find the lowest oxygen concentration in an upward flowing mixture of nitrogen and oxygen which just supports sustained burning. Specimen dimensions for the OI measurement were 100 × 10 × 10 mm (length × width × thickness).

2.3.4. Thermal conductivity of PIR composite foams

Thermal conductivity is the rate of steady-state heat flow (*W*) through a unit area of a 1 m thick homogeneous material, in a direction perpendicular to the isothermal plane, induced by a unit (1 K) temperature difference across the sample [1]. Thermal conductivity tests of different PIR foams were measured using a thermal conductivity analyzer (JW-III) as per Chinese standard GB/T 3399-82. The size of the specimen was 25 × 25 × 2 cm.

2.3.5. Fourier transform infrared (FTIR) spectroscopy

FTIR spectrophotometric analyses were performed to determine the structure of the PIR foams using a Nicolet 5700 FTIR spectrometer. Typically, 100 scans over the range of 4000–400 cm^{-1} were performed for each sample with a resolution of 2 cm^{-1}.

2.3.6. Scanning electron microscope (SEM) studies of PIR composite foams

An SEM equipped with an energy dispersive X-ray detector (EVO 18) at an accelerating voltage of 5 kV was used to observe the dispersion and morphology of RPUFs/granular silica aerogel composites. The surface of the foam sample was coated with a thin layer of gold before analysis.

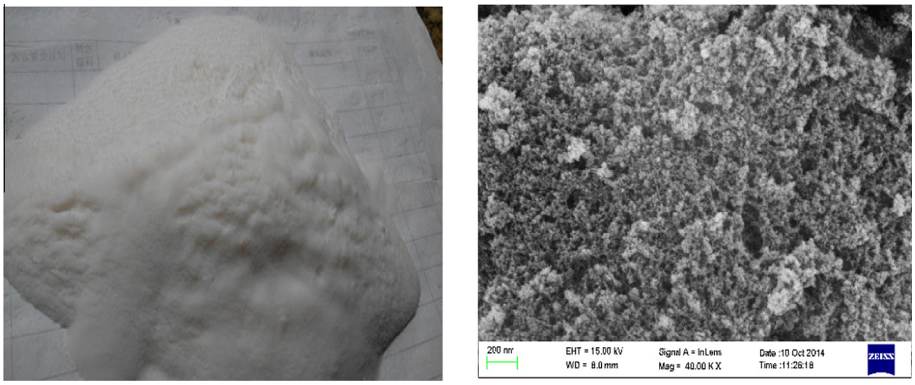

Fig. 1. Macroscopic (left) and microscopic (right) images of granular silica aerogel.

3. Results and discussion

3.1. Mechanical performance of PIR composite foams

Considering their practical use, the compressive strength of PIR foams is a critical property. PIR foams were prepared using different polyols mixed as shown in Table 1. The effect of the proportion of silica aerogel on compressive strength and specific strength (the ratio of compressive strength to bulk density) of PIR foam/granular aerogel composites is presented in Fig. 2.

Fig. 2(a1 and b1) shows that the compressive strength of the composites was increased with addition of silica aerogel. Compressive strength increased at first and then fell as the proportion of aerogel increased. When the proportion of silica aerogel reached 3 wt.% in matrix A (Fig. 2(a1 and a2)), both the compressive and specific strengths of the composite were at their maximum values. Compared with control PIR foam, the compressive strength of the composites increased by 11.6%. The silica aerogel particles easily aggregate in this matrix when the proportion of aerogel exceeds 3 wt%. For composites prepared from matrix B (Fig. 2(b1 and b2)), the compressive and specific strengths of the composite containing 3 wt.% aerogel were relatively low compared with the corresponding composite prepared from matrix A. However, when the proportion of silica aerogel was increased to 6 wt.%, both the compressive and specific strengths of the composite reached their maximum values. The compressive and specific strengths of the composite were enhanced by 136% and 92.2%, respectively, compared with the control foam. The performance of the composites declined when the proportion of aerogel exceeded 6 wt.%. These results suggest that a low viscosity polyol system (matrix B) is beneficial to the dispersion of granular silica aerogel when the proportion is less than that required to maximize compressive and specific strengths. When the proportion of silica aerogel is increased beyond this level, the mechanical properties of the composites began to decline due to the higher viscosity of the matrix (matrix A) leading to uneven dispersion of the silica aerogel particles. This phenomenon weakens the mechanical properties of the composites by hindering the interaction of the nanomaterials with PU macromolecules [24]. The physico-mechanical properties of PIR foams are also dependent on the rigidity of the polymer matrix and the cell morphology of the foams. Thus, it is of interest to observe changes to the internal structure of the foam specimen using SEM [25].

Table 1
The formula of PIR composites foam with granular silica aerogel.

Formula	Compressive strength	Specific strength
A: polyether 4110 and polyester PS3152 mixed	a1	a2
B: PEG 600 mixed	b1	b2

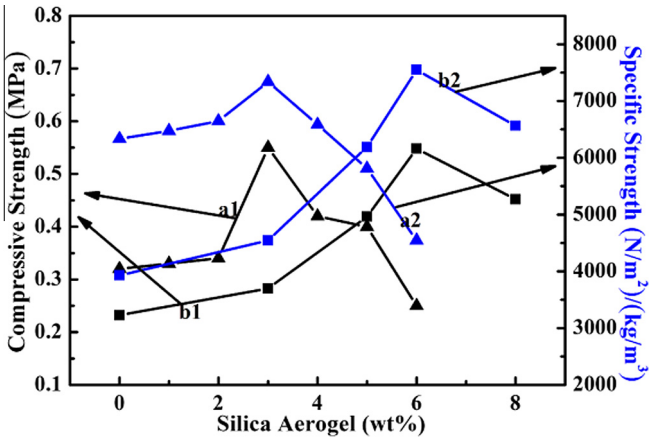

Fig. 2. Compressive strength (a1 and b1) and specific strength (a2 and b2) of composites with varying silica aerogel content.

3.2. TGA

TGA helps to determine the maximum temperature that the material can withstand without decomposition. The objective of the analyses was to profile the decomposition characteristics of the composite foams.

As seen in Fig. 3(a) and (b), composite foams had better heat resistance properties compared with the control PIR foam. With increasing silica aerogel content, the heat resistance of the composites was gradually improved. The residue after heating at 800 °C (Fig. 3(a)) increased from 24.13% at 0 wt.% aerogel to 38.06% at 6 wt.% aerogel. The initial thermal decomposition temperature of the composite foams was increased by 70 °C compared with the control PIR foam. The corresponding residues for composites shown in Fig. 3(b) were 27.2% at 0 wt.% aerogel and 47.6% at 8 wt.% aerogel after heating at 800 °C. The residual amounts for the PIR composite foams in Fig. 3(b) were higher than those in Fig. 3(a). These results suggest that incorporation of silica aerogel particles can help to improve the thermal stability of the organic foams. This can be attributed to the high thermal performance of the silica aerogel, which acts as a barrier to prevent rapid heat dispersal and limits further degradation. Silica aerogel, as an inorganic filler, can act as a physical or chemical cross-linking agent to

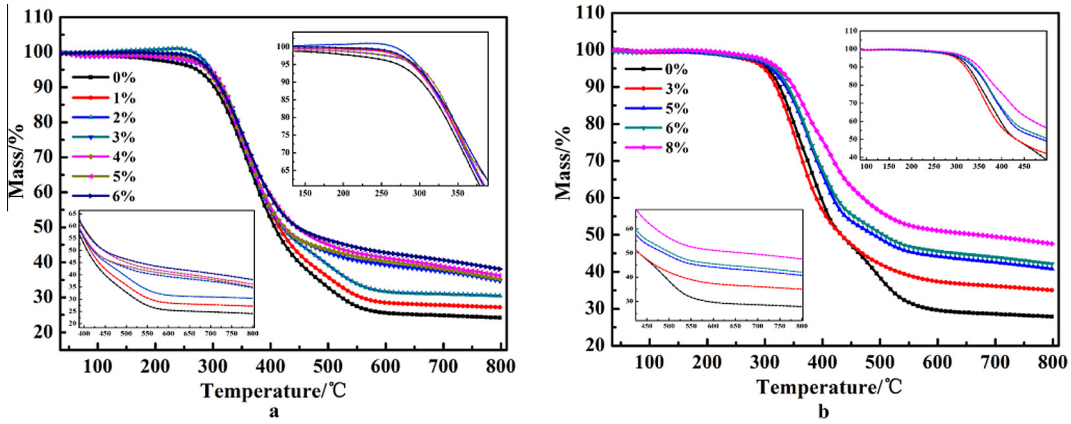

Fig. 3. TG curves of composites with varying silica aerogel content.

improve the cross-link density of PIR foam, restricting mobility of the polyurethane molecular chains. Introduction of Si–O, with strong combining ability, into the PU C–C network results in greater heat resistance of these organic/inorganic composites compared with control PIR foams. These composites are therefore very promising as thermal insulation materials [22].

3.3. Flame retardant properties of PIR composites: OI

OI, which describes the ease with which an organic material can sustain a flame, is widely used as a tool to characterize the flammability of polymers. The effect of the proportion of silica aerogel on the flame retardant properties of PIR foam/granular aerogel composites is presented in Fig. 4.

Overall, the OI of the composites gradually increased as the proportion of silica aerogel increased. The OI increased from 27.2% to 31.0% at 0 wt.% and 6 wt.% aerogel, respectively, in Fig. 4(a) and from 29.4% to 34.6% at 0 wt.% and 8 wt.% aerogel, respectively, in Fig. 4(b). The presence of granular silica aerogel leads to an increased OI of the PIR composite foam that is higher than that of conventional RPUF (OI: 22–24%). Based on these analyses, the OI values of the low viscosity system PIR foam composites are relatively much higher compared with the high viscosity system composites and the control PIR foam. This suggests that the flame retardant properties of PIR foams are improved when a large amount of inorganic material is incorporated. This may be because silica aerogel is one of the best thermal insulation materials and its thermal endurance properties prevent the rapid transfer of heat. In addition, inclusion of silica aerogel dilutes the proportion of combustible material, which increases the flame retardant properties of the composite foams [26]. Silica aerogels, as thermal insulators, can be used as inorganic fillers, providing a barrier layer to inhibit combustion.

3.4. Thermal conductivity of PIR composites

Thermal conductivity was measured using a special hot plate device designed for small samples of low conductivity materials. The thermal conductivity of the PIR foams is an important parameter as an indicator of thermal insulation properties. The effect of the proportion of silica aerogel on the thermal conductivity of PIR foam/granular aerogel composites is presented in Fig. 5.

From Fig. 5, it can be seen that the thermal conductivity of the composite foams decreased as the proportion of silica aerogel increased. When the proportion of silica aerogel was increased to 6 wt.% in composites prepared from matrix A, the thermal conductivity was reduced by 30.2% (Fig. 5(a)). In composites prepared from matrix B, thermal conductivity was reduced by 32.7% (from 0.0346 W/(m K) at 0 wt.% aerogel to 0.0233 W/(m K) at 8 wt.% aerogel) as shown in Fig. 5(b). This effect results from the very low thermal conductivity of silica aerogel itself (<0.02 W/(m K)) and the good bubble pore structure of the composite foams. The results indicate that the thermal insulation properties of the composites are improved compared with control PIR foams.

In general, the thermal conductivity of RPUF depends on foam density, cell size, pore connectivity, and the ratio of closed to open cells [21]. As seen by SEM (Fig. 7), PIR foam composites maintain a bubble pore structure, with an ordered arrangement of small cells.

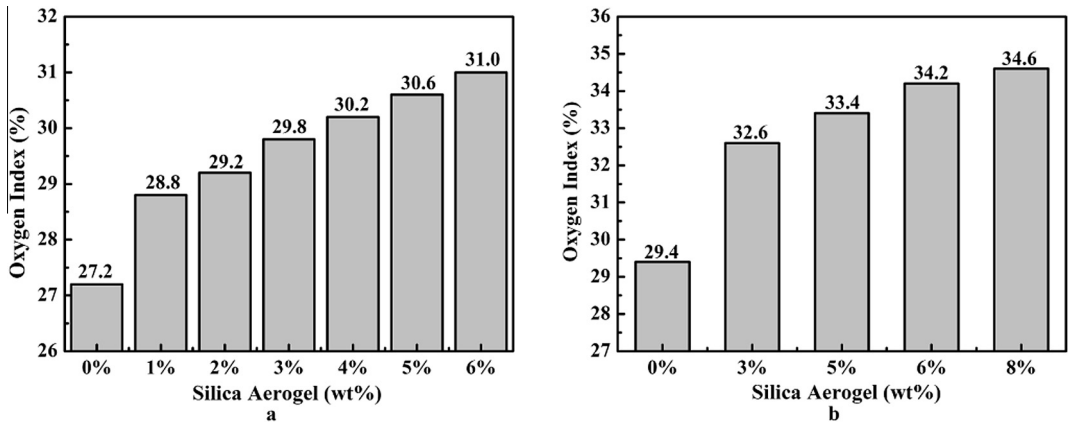

Fig. 4. Oxygen indexes of composites with varying silica aerogel content.

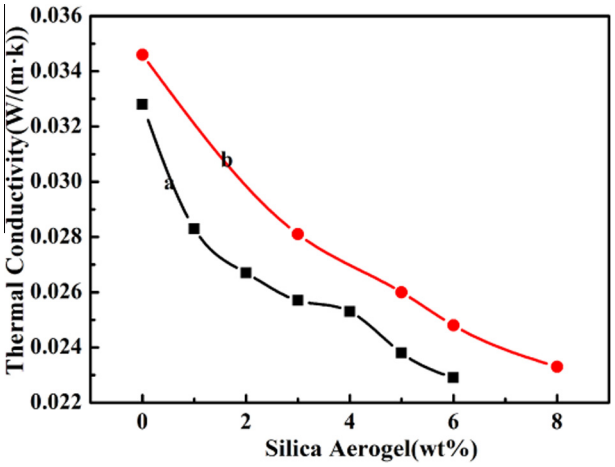

Fig. 5. Thermal conductivity of composites with varying silica aerogel content.

This is advantageous since reducing cell size is a method to improve thermal insulation properties. In addition, the bulk density of granular silica aerogel is low, with high porosity, both of which properties help to reduce thermal conductivity.

3.5. FTIR analyses of control PIR and composites

The influence of granular silica aerogel on the internal structure of PU was as follows: Fig. 6(a_0) shows the FTIR spectrum of conventional RPUFs; Fig. 6(a) shows the FTIR spectra of composites in the matrix A with varying silica aerogel content: (a) 0 wt.%, (b) 1 wt.%, (c) 2 wt.%, (d) 3 wt.%, (e) 4 wt.%, (f) 5 wt.%, (g) 6 wt.%; Fig. 6(b) shows the FTIR spectra of composites in the matrix B with varying silica aerogel content: (a) 0 wt.%, (b) 3 wt.%, (c) 5 wt.%, (d) 6 wt.%, (e) 8 wt.%.

The assignments of infrared absorption bands to functional groups in the control PIR foam are shown in Table 2. As shown in Fig. 6, the absence of the isocyanate stretch at 2275 cm^{-1} in the composites indicates that the isocyanate groups have completely reacted. The band at 1712 cm^{-1}, which represents the stretching vibration of carbonyl groups hydrogen-bonded between the N–H and C=O of urethane linkages, indicates the formation of inter-urethane hydrogen bonding. The results suggest that PU is a complex mixture containing hydroxyl and other active functional groups (carbonyl groups, aromatic rings and ether bonds) [27–29].

FTIR spectra of the composite foams with different amounts of silica aerogel are shown in Fig. 6(a) and (b). The relative positions of the distinctive peaks for the different functional groups in the composites are identical to those of the control PIR foams, indicating that the segmented structure of PIR has not been disturbed by the presence of granular silica aerogel. The main characteristic peaks were unchanged [30]. This suggests that the bonding in granular silica aerogel particles does not participate in the reaction. Additionally, inclusion of silica aerogel particles does not change the chemical structure of PIR.

Table 2
FTIR band assignments to functional groups.

Wavenumber (cm^{-1})	Functional groups
3369	—NH— stretching vibration absorption
2913	C—H stretching
2275	—N=C=O antisymmetric stretching
1712	C=O stretching vibration
1596	Benzene rings C=C stretching
1225	C—O asymmetry stretching
1068	C—O—C asymmetry stretching in alcohol hydroxyl
814	=C—H variable angle vibration in benzene ring

3.6. SEM analysis

Cell morphology is very important in determining the thermal conductivity and mechanical properties of rigid PIR foam. Fig. 7 shows SEM photos of PIR composites in the matrix A with varying silica aerogel content, magnified 200 times. The proportions of silica aerogel are: (a) 0 wt.%, (b) 1 wt.%, (c) 2 wt.%, (d) 3 wt.%, (e) 4 wt.%, (f) 5 wt.%, (g) 6 wt.%. These images enable observation of the bubble structure, bubble hole distribution and bubble defects.

As shown in Fig. 7, the bubble hole shape of the control PIR foam is not very uniform. The composites have smaller bubble pore structure, greater bubble hole density and better mechanical performance compared with control PIR foam. Addition of appropriate quantities of aerogel provides composites with better pore structure and ordered bubble arrangement. However, when the proportion of silica aerogel particles is high, the matrix viscosity in the system will be high, leading to uneven mixing. This phenomenon makes uniform dispersion difficult and stretches the bubble pores as a result of altered mixing dynamics. Under these conditions the mechanical properties of the composites will be compromised because the skeleton structure is damaged.

Fig. 8 shows SEM images of PIR composites in the matrix B with varying silica aerogel content. The proportions of silica aerogel are: (a) 0 wt.%, (b) 3 wt.%, (c) 5 wt.%, (d) 6 wt.%, (e) 8 wt.%.

Fig. 8(a) shows that the control PIR foam has fewer cells and a larger cell size compared with PIR composite foams. The pore structure of the cell has some serious destruction and collapse of the cell system. It is also apparent that the reduced functionality diminishes the crosslink density of the polyurethane macromolecules, which results in degradation of mechanical performance. It can be seen from the other images that the cell shapes

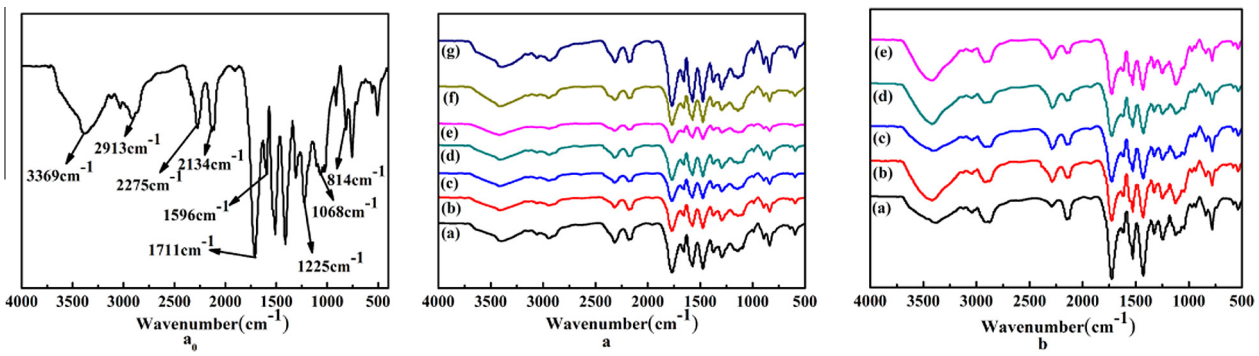

Fig. 6. FTIR spectra of composites with varying silica aerogel content.

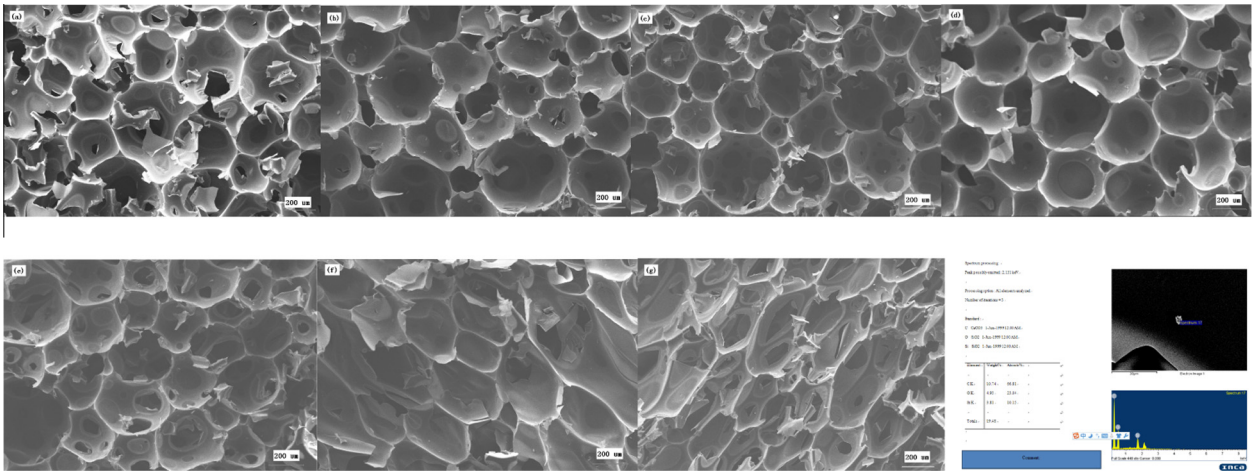

Fig. 7. SEM images of composites with varying silica aerogel content.

are approximately spherical polyhedral and symmetrical in the PIR composite foams filled with granular silica aerogel. All foams exhibit polygon closed-cell structures with energetically-stable pentagonal and hexagonal faces. As shown in Fig. 8(b–d), the introduction of granular silica aerogel can effectively reduce the cell size and form more compact structures compared with the control PIR foam. The SEM results indicate that PIR composite foams have improved cell size due to the presence of granular silica aerogel. These results suggest that the nature of the dispersion plays a vital role in controlling the size of the cell during foaming [12]. The compact cell structure of the composite foams compared with control PIR foam may be due to the uniform dispersion of granular silica aerogel within the PIR foam without any cracks, preserving matrix cross-linking, even if there are some holes in the thin cell wall due to local internal stress or unbalanced foam growth [13]. It appears that further incorporation of silica aerogel does not change the cell shape, but alters homogeneity of the PIR foam.

3.7. Properties of PIR foam composites with silica aerogel and waste residue

When the proportion of silica aerogel was 3 wt.%, all properties and the bubble pore structure of composite foams in the matrix A with varying silica aerogel content were relatively good. However, because of the higher viscosity of the system, the proportion of granular silica aerogel could not be increased further without compromising performance. In contrast, all properties of composite foams in the matrix B with varying silica aerogel content were better than those of the abovementioned composite foams when the proportion of silica aerogel was 6 wt.%. The lower viscosity of the system permitted a higher proportion of silica aerogel. In order to reduce costs, we explored the use of waste residue polyols to

Table 3
Effects of silica aerogel and waste residue on PIR composite foams.

Performance characterization	Compressive strength (MPa)	Specific strength (N/m^2)/(kg/m^3)	TG (%)	OI (%)	Thermal conductivity (W/(m K))
Control PIR foams	0.232	3926.9	27.2	29.4	0.0346
Composites foam with waste residue	0.22	3636.4	36.5	30.8	0.0296
Composites foam with 6% silica aerogel and waste residue	0.291	4789.4	44	34.4	0.0251

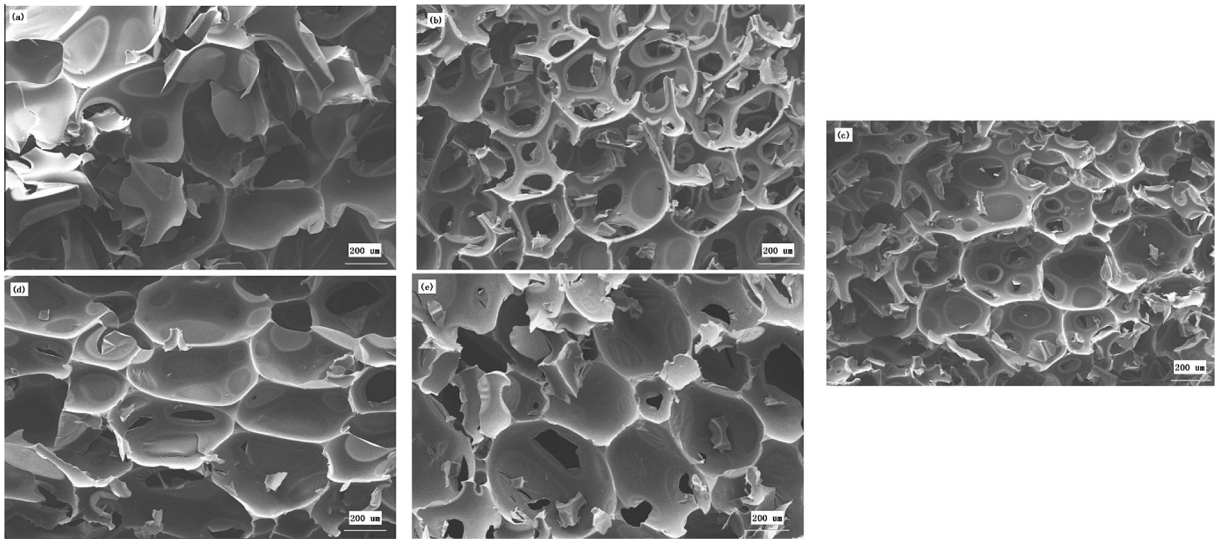

Fig. 8. SEM images of PIR composite foams prepared with PEG 600 containing different proportions of silica aerogel.

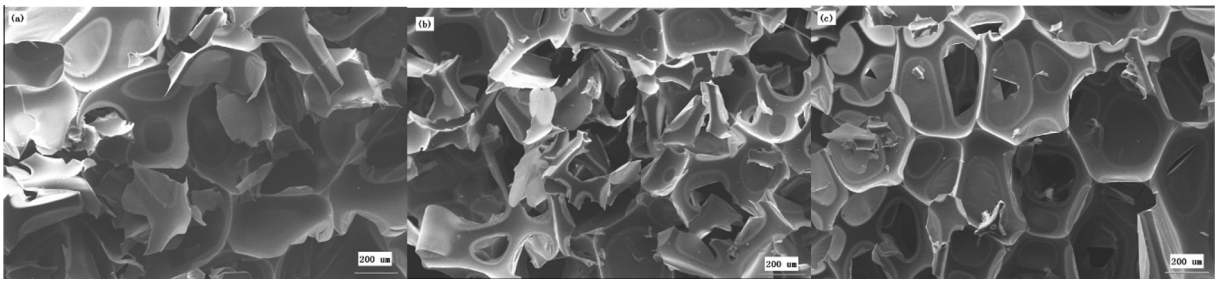

Fig. 9. SEM images showing the effects of granular silica aerogel and waste residue on PIR composite foams.

prepare composite foams with silica aerogel. Comparative results are shown in Table 3.

The effects of granular silica aerogel and waste residue on the SEM of PIR composite foams are shown in Fig. 9: (a) is control PIR foam; (b) is composite foam prepared with waste residue; (c) is composite foam with 6 wt.% silica aerogel and waste residue.

Waste residue is a by-product from the preparation of 1,4-butanediol, which is a complex of polymer polyols with a carbon layer. From the data above, the strength of the foams with waste residue was slightly reduced. Further, the SEM image in Fig. 9 shows that the cell structure does not have the support of a skeleton. However, all properties were significantly enhanced by the addition of silica aerogel particles. The results illustrate that composite foams with silica aerogel and waste residue have better performance at lower cost. The significant improvement may be attributed to the higher hydroxyl value of waste residue. The dominant effect is the extremely high cross-link density (from the reaction of a larger number of hydroxyls with isocyanate groups). Waste residue polyols with a carbon layer can effectively promote char formation at this temperature and the char protects and retards further decomposition of the PIR beneath it. At higher temperatures it forms a carbonaceous residue that enhances flame retardant properties. The char-forming ability can lead to the formation of char layers with excellent thermal insulation, protecting the inner part of the material from fire [27,28].

4. Conclusions

PIR composite foams have been prepared and characterized in this study. Considerable research has shown that the addition of waste residue polymer polyols and granular silica aerogel in matrix B can significantly improve both the flame retardant and heat insulation properties of PIR foams. The OI was increased to 34.6% at 8 wt.% aerogel from 29.4% at 0 wt.% aerogel. The thermal conductivity of the PIR foam composites was reduced by 32.7% (from 0.0346 W/(m K) at 0 wt.% aerogel to 0.0233 W/(m K) at 8 wt.% aerogel). The compressive strength of the composites was enhanced by 136% compared with the control foam. The specific strength was enhanced by 92.2% using PEG 600 as the polyol source. The TGA results revealed that the corresponding weight losses were lower than that of control PIR foam. The pore structure of the cell was effectively improved by the addition of silica aerogel particles.

Acknowledgments

The authors acknowledge the financial support of the National High-Tech. R&D Program (863program) (No. 2011AA06A106) of China, the Open Project of State Key Laboratory Cultivation Base for Non-metal Composites and Functional Materials (No. 11zxfk26), and we thank the administrators of the fund for their support in our research.

References

[1] Al-Homoud MS. Performance characteristics and practical applications of common building thermal insulation materials. Build Environ 2005;40(3):353–66.
[2] Lu W, Ma Y. Image of energy consumption of well off society in China. Energy Convers Manage 2004;45(9–10):1357–67.
[3] Cai WG, Wu Y, Zhong Y, Ren H. China building energy consumption: situation, challenges and corresponding measures. Energy Policy 2009;37(6):2054–9.
[4] Fang Zhaosong, Li Nan, Li Baizhan, Luo Guozhi, Huang Yanqi. The effect of building envelope insulation on cooling energy consumption in summer. Energy Build 2014;77:197–205.
[5] Kaynakli Omer. A review of the economical and optimum thermal insulation thickness for building applications. Renew Sustain Energy Rev 2012;16:415–25.
[6] Pilkington Brian, Grove Stephen. Thermal conductivity probe length to radius ratio problem when measuring building insulation materials. Constr Build Mater 2012;35:531–46.
[7] Jelle Bjørn Petter. Traditional, state-of-the-art and future thermal building insulation materials and solutions – properties, requirements and possibilities. Energy Build 2011;43:2549–63.
[8] Dylewski Robert, Adamczyk Janusz. Economic and environmental benefits of thermal insulation of building external walls. Build Environ 2011;46:2615–23.
[9] Chen Xilei, Huo Lili, Jiao Chuanmei, Li Shaoxiang. TG-FTIR characterization of volatile compounds from flame retardant polyurethane foams materials. J Anal Appl Pyrol 2013;100:186–91.
[10] Zhang XB, Yao L, Qiu LM, Gan ZH, Yang RP, Ma XJ, et al. Experimental study on cryogenic moisture uptake in polyurethane foam insulation material. Cryogenics 2012;52(12):810–5.
[11] Van Nieuwenhuyse AvE. Thermal insulation materials made of rigid polyurethane foam (PUR/PIR). Properties-manufacture 2006; 6: 1–33.
[12] Nikje Mir Mohammad Alavi, Tehrani Zahra Mazaheri. Thermal and mechanical properties of polyurethane rigid foam/modified nanosilica composite. Polym Eng Sci 2010.
[13] Zhang Liqiang, Zhang Meng, Zhou Yonghong, Hu Lihong. The study of mechanical behavior and flame retardant of castor oil phosphate-based rigid polyurethane foam composites containing expanded graphite and triethyl phosphate. Polym Degrad Stab 2013;98:2784–94.
[14] Chattopadhyay DK, Webster Dean C. Thermal stability and flame retardant of polyurethanes. Prog Polym Sci 2009;34:1068–133.
[15] Beyer G. Filled blend of carbon nanotubes and organoclays with improved char as a new flame retardant system for polymers and cable applications. Fire Mater 2005;29(2):61–9.
[16] Thirumal M, Khastgir D, Singha NK, Manjunath BS, Naik YP. Effect of expandable graphite on the properties of intumescent flame-retardant polyurethane foam. J Appl Polym Sci 2008;110:2586–94.
[17] Gao Xiaoyan, Zhou Bing, Guo Yupeng, Zhu Yanchao, Chen Xue, Zheng Yunhui, et al. Synthesis and characterization of well-dispersed polyurethane/$CaCO_3$ nanocomposites. Colloids Surf A 2010;371:1–7.
[18] Vassiliou AA, Chrissafis K, Bikiaris DN. In situ prepared PET nanocomposites: effect of organically modified montmorillonite and fumed silica nanoparticles on PET physical properties and thermal degradation kinetics. Thermochim Acta 2010;500(1–2):21–9.
[19] Gao Liping, Zheng Guangyao, Zhou Yonghong, Hu Lihong, Feng Guodong, Zhang Meng. Synergistic effect of expandable graphite, diethyl ethylphosphonate and organically-modified layered double hydroxide on flame retardant and fire behavior of polyisocyanurate-polyurethane foam nanocomposite. Polym Degrad Stab 2014;101:92–101.
[20] Kango Sarita, Kalia Susheel, Celli Annamaria, Njuguna James, Habibi Youssef, Kumar Rajesh. Surface modification of inorganic nanoparticles for development of organic–inorganic nanocomposites – a review. Prog Polym Sci 2013;38:1232–61.
[21] Zhang Yahong, Huo Yanli, Kalantar Thomas H. Inorganic nanoporous particles with water dispersible polyurethane binder [P]US2013/0091682Al.2013-04-18.
[22] Baetens Ruben, Jelle Bjørn Petter, Gustavsend Arild. Aerogel insulation for building applications: a state-of-the-art review. Energy Build 2011;43:761–9.

[23] Feng Junjie, Zhang Ruifang, Gong Lunlun, Li Ye, Cao Wei, Cheng Xudong. Development of porous fly ash-based geopolymer with low thermal conductivity. Mater Des 2015;65:529–33.
[24] Mar Bernal M, Martin-Gallego Mario, Romasanta Laura J, Mortamet Anne-Cecile, López-Manchado Miguel A, Ryan Anthony J, et al. Effect of hard segment content and carbon-based nanostructures on the kinetics of flexible polyurethane nanocomposite foams. Polymer 2012;53:4025–32.
[25] Piszczyk Łukasz, Strankowski Michał, Danowska Magdalena, Haponiuk Józef T, Gazda Maria. Macromolecular nanotechnology preparation and characterization of rigid polyurethane–polyglycerol nanocomposite foams. Eur Polymer J 2012;48:1726–33.
[26] Lichung Chang, Yu Xue, Fu-Hung Hsieh. Dynamic-mechanical study of water-blown rigid polyurethane foams with and without soy flour. J Appl Polym Sci 2001;81:2027–35.
[27] Pradhan KC, Nayak P. Synthesis and characterization of polyurethane nanocomposite from castor oil-hexamethylene diisocyanate (HMDI). Adv Appl Sci Res 2012;3(5):3045–52.
[28] Pauzi Nik Nurfatmah Pz Nik, Majid Rohah A, Dzulkifli Mohd Haziq, Yahya Mohd Yazid. Development of rigid bio-based polyurethane foam reinforced with nanoclay. Compos B Eng 2014;67:521–52.
[29] Zou Xianwu, Qin Tefu, Wang Yong, Huang Luohua, Han Yanming, Li Yan. Synthesis and properties of polyurethane foams prepared from heavy oil modified by polyols with 4,4-methylene-diphenylene isocyanate (MDI). Bioresour Technol 2012;114:654–7.
[30] Saha MC, Kabir MdE, Jeelani S. Enhancement in thermal and mechanical properties of polyurethane foam infused with nanoparticles. Mater Sci Eng A 2008;479:213–22.